© 2014. Published by The Company of Biologists Ltd | Journal of Cell Science (2014) 127, 5228–5239 doi:10.1242/jcs.154393

RESEARCH ARTICLE

Delivery of CSF-1R to the lumen of macropinosomes promotes its destruction in macrophages

Jieqiong Lou, Shalini T. Low-Nam, Jason G. Kerkvliet and Adam D. Hoppe*

ABSTRACT

Activation of the macrophage colony stimulating factor-1 receptor (CSF-1R) by CSF-1 stimulates pronounced macropinocytosis and drives proliferation of macrophages. Although the role of macropinocytosis in CSF-1R signaling remains unknown, we show here that, despite internalizing large quantities of plasma membrane, macropinosomes contribute little to the internalization of the CSF-1–CSF-1R complex. Rather, internalization of the CSF-1R in small endocytic vesicles that are sensitive to clathrin disruption, outcompetes macropinosomes for CSF-1R endocytosis. Following internalization, small vesicles carrying the CSF-1R underwent homotypic fusion and then trafficked to newly formed macropinosomes bearing Rab5. As these macropinosomes matured, acquiring Rab7, the CSF-1R was transported into their lumen and degraded. Inhibition of macropinocytosis delayed receptor degradation despite no disruption to CSF-1R endocytosis. These data indicate that CSF-1-stimulated macropinosomes are sites of multivesicular body formation and accelerate CSF-1R degradation. Furthermore, we demonstrate that macropinocytosis and cell growth have a matching dose dependence on CSF-1, suggesting that macropinosomes might be a central mechanism coupling CSF-1R signaling and macrophage growth.

KEY WORDS: CSF-1R, M-CSF, Endocytosis, Macrophage, Macropinosome

INTRODUCTION

Following stimulation by extracellular ligands, transmembrane receptor tyrosine kinases (RTKs) initiate signaling cascades that ultimately impact upon cellular metabolism and growth (Lemmon and Schlessinger, 2010). Clearance of RTKs from the plasma membrane by small endocytic vesicles, including those involved in clathrin-mediated endocytosis (CME), is a primary mechanism for attenuating RTK mitogenic signals (Polo and Di Fiore, 2006; Sorkin and von Zastrow, 2009; von Zastrow and Sorkin, 2007). RTKs such as the epidermal growth factor receptor (EGFR) are targeted to clathrin-coated pits by a combination of signals that include ubiquitylation (Goh et al., 2010). RTK-containing endosomes mature by fusing sequentially with membranes of the early endosome, late endosome and the lysosome, leading to RTK degradation. Alternatively, the RTK can be delivered to recycling endosomes and returned to the cell surface (Sorkin and Goh, 2009). Ubiquitylated RTKs are generally targeted for degradation through the endosomal sorting complex required for transport (ESCRT) machinery, which packages them into vesicles that bud into the lumen of the late endosome to form a multivesicular body (MVB) (Hurley and Emr, 2006). These two activities of RTK degradation and recycling modulate RTK signals, highlighting the complexity of membrane traffic as route for activating and terminating signaling (Huynh et al., 2012; Polo and Di Fiore, 2006; Porat-Shliom et al., 2008; Sigismund et al., 2008; Sorkin and von Zastrow, 2009; Valdez et al., 2007).

Many RTKs stimulate actin-driven membrane ruffling and the formation of macropinosomes, which mediate the internalization of large quantities of extracellular fluid and plasma membrane (Kerr and Teasdale, 2009; Swanson, 2008). Following membrane scission, different trafficking fates are possible for macropinosomes. In macrophages, CSF-1R-stimulated macropinosomes mature by acquiring Rab5 and Rab7, marking them as early and late endosomes, respectively, prior to fusion with the lysosome (Feliciano et al., 2011; Racoosin and Swanson, 1993). Alternatively, EGF stimulation of A431 cells leads to the formation of macropinosomes that do not mature to form endosomes, but eventually fuse back with the plasma membrane (Hewlett et al., 1994; Kerr and Teasdale, 2009). Although the exact function of macropinocytosis in RTK signaling remains unknown, a number of RTKs, such as tropomyosin receptor kinases (Trks) and platelet-derived growth factor receptors (PDGFRs) (Philippidou et al., 2011; Porat-Shliom et al., 2008; Schmees et al., 2012; Valdez et al., 2005; Valdez et al., 2007) have been reported to localize to macropinosomes, where they are thought to signal. Importantly, macropinosomes have been implicated in the uptake of nutrients such as extracellular protein in Ras-transformed cancer cells (Commisso et al., 2013) and in the axenic mutants of *Dictyostelium* (Clarke and Kayman, 1987; Veltman et al., 2014). Macropinosomes have also been ascribed other non-RTK functions, such as antigen sampling by dendritic cells (Norbury, 2006) and the internalization of viruses (Mercer et al., 2010). Thus, macropinosomes play diverse and as yet poorly defined roles, some of which are downstream of RTK signaling.

Although the signal transduction downstream of the CSF-1R is well-defined, the mechanisms of its clearance from the cell surface remain poorly characterized. Extensive biochemical characterization has shown that the CSF-1R signals through the Ras–MAPK–Erk, Jak–STAT and Akt–PI3K pathways to control macrophage proliferation, differentiation and chemotaxis (Lee et al., 1999; Pixley and Stanley, 2004; Wang et al., 1999; Xiong et al., 2011; Yeung et al., 1998; Yu et al., 2008; Yu et al., 2012). CSF-1 potently stimulates macropinocytosis in macrophages in a phosphoinositide 3-kinase (PI3K)- and Rac1-dependent manner (Araki et al., 1996; Boocock et al., 1989; Fujii et al., 2013; Racoosin and Swanson, 1992). Additionally, signals downstream of the CSF-1R, including PI3K products, activated Rac1 and Ras,

Department of Chemistry and Biochemistry, South Dakota State University, Brookings, 57007 SD, USA.

*Author for correspondence (adam.hoppe@sdstate.edu)

Received 3 April 2014; Accepted 8 October 2014

Journal of Cell Science

Journal of Cell Science (2014) 127, 5228–5239 doi:10.1242/jcs.154393

have been reported to localize to forming macropinosomes (Feliciano et al., 2011; Welliver et al., 2011; Yoshida et al., 2009). However, the distribution of receptors relative to this structure has not previously been mapped, nor has the mechanism of CSF-1R internalization been defined. Thus far, CSF-1R has been observed to be internalized by small vesicles, which are thought to fuse to form large endosomal structures (Boocock et al., 1989; Murray et al., 2000) where CSF-1R is ultimately degraded (Chen and Lin, 1984). The importance of understanding the interplay between CSF-1R signaling and traffic was highlighted recently by the finding that endocytosis of the CSF-1R mediates sustained Erk and Akt signaling that is necessary for transcriptional activities associated with macrophage growth (Huynh et al., 2012).

Here, we define the internalization and intracellular transport of the CSF-1R in macrophages. We find that macropinosomes contribute little to the internalization of the CSF-1R. Instead, small endocytic vesicles that are sensitive to clathrin inhibition internalize the CSF-1R, undergo homotypic fusion and then traffic to Rab5-labeled macropinosomes where they mature into Rab7-positive compartments. The receptor is subsequently transported into the macropinosome lumen, consistent with MVB formation, where it is degraded. These data demonstrate that CSF-1R-stimulated macropinosomes regulate the CSF-1R, thereby coupling the capture of extracellular solutes through macropinocytosis with CSF-1R-mediated cell growth.

RESULTS

CSF-1 stimulates the production of macropinosomes at mitogenic concentrations and is delivered to their lumen

Exposure of bone-marrow-derived macrophages (BMM) to CSF-1 increases the number and volume of macropinosomes as measured by the uptake of Texas-Red–dextran (TXR–Dex; 70,000 Da) (Fig. 1A,B; supplementary material Movie 1; Racoosin and Swanson, 1992). From these data, we estimate that 10% of the macrophage plasma membrane was internalized (neglecting exocytic events) during the first 5 minutes of exposure to CSF-1. The large surface area internalized by macropinocytosis in response to CSF-1 and the colocalization between CSF-1–CSF-1R and large endocytic compartments (Boocock et al., 1989; Murray et al., 2000) led us to consider the possibility that that macropinosomes facilitate internalization of the activated CSF-1R.

To test this possibility, we made functional Texas-Red–CSF-1 (TXR–CSF-1; supplementary material Fig. S1). Surprisingly, live-cell imaging of CSF-1-starved BMMs showed that TXR–CSF-1 was internalized in small (<500-nm diameter) endosomes (Fig. 1C; supplementary material Movie 2) within 2–5 minutes following stimulation. Macropinosomes (>500-nm diameter) formed during this time; however, when first formed, they did not enrich TXR–CSF-1 above plasma membrane levels (Fig. 1C, arrow at 5 minutes). After ~5 minutes, the small vesicles containing TXR–CSF-1 were delivered to macropinosomes in a two-step process. First, the small endosomes containing TXR–CSF-1 fused into slightly larger and brighter vesicles that were trafficked to patches on the limiting membrane of the macropinosome (Fig. 1C, arrow at 8 minutes; supplementary material Movie 2). In a second step, the TXR–CSF-1 was transported into the macropinosome lumen, which could then be visualized as a large fluorescent sphere containing TXR–CSF-1 (Fig. 1C, arrow at 11 minutes; supplementary material Movie 2). By exposing cells to a fluid-phase marker (Lucifer Yellow) and TXR–CSF-1 we verified that these were indeed macropinosomes and not pre-existing late endosomes (supplementary material Fig. S2; Movie 3). Thus, during acute CSF-1 exposure, macropinosomes are not a major endocytic route for the CSF-1R; rather, they are a destination for the CSF-1R following internalization of small vesicles.

To confirm that the CSF-1R trafficked to macropinosomes as predicted by watching TXR–CSF-1, we devised a sequential immunofluorescence procedure to visualize the CSF-1R and the macropinosome lumen marked by TXR–Dex. This sequential staining procedure was necessary, because TXR–Dex or lysine-fixable TXR–Dex would leak out from the macropinosome upon permeabilization, leaving only a weak label on the limiting membrane of the macropinosome. Following a 5-minute pulse with CSF-1 and a 10-minute chase, macrophages were fixed and imaged. Macropinosomes appeared as fluorescent spheres (Fig. 1D, left panel). The macropinosome coordinates were recorded using a robotic stage and the cells were then permeabilized, resulting in loss of TXR–Dex fluorescence as the macromolecules leaked out (Fig. 1D, center panel). Subsequent immunodetection of CSF-1R revealed that, on average, three out of four macropinosomes contained the CSF-1R and about half of all new macropinosomes showed punctate CSF-1R structures in their lumen (Fig. 1D, right panel; Fig. 1E). Indeed, 15 minutes following CSF-1 exposure, macropinosomes could be readily identified in macrophages by their accumulation of the CSF-1R (supplementary material Fig. S3).

Macropinosomes have been regarded as possible routes for nutrient uptake for catabolism (Commisso et al., 2013; Veltman et al., 2014), implying that CSF-1 might drive macropinocytosis to promote growth by facilitating nutrient uptake. To determine whether macropinocytosis and cell growth are regulated downstream of the CSF-1R, we measured macropinosome number and BMM growth during continuous exposure to a range of CSF-1 concentrations. Indeed, macropinosome number and cell number increased in an identical CSF-1 dose-dependent manner (Fig. 1F). Moreover, acute exposure to physiological concentrations of ~5 ng/ml CSF-1 (Scholl et al., 1994) caused the CSF-1R to traffic to macropinosomes (Fig. 1G). These results demonstrate that macropinocytosis is not an artifact of high levels of acute exposure to CSF-1 and that cell growth and macropinocytosis are coupled downstream of CSF-1R at all concentrations that support BMM growth.

The delivery of the CSF-1R to the macropinosome was not unique to murine BMMs. Exposure of human monocyte-derived macrophages (hMDM) to CSF-1 induced macropinocytosis and trafficking of TXR–CSF-1 to macropinosomes. Thus, this mechanism is conserved across human and mouse macrophages (Fig. 1H,I).

To test whether the activated CSF-1R was transported into the macropinosome lumen, we devised a strategy for staining cytosolic and extracellular epitopes on the CSF-1R while specifically permeabilizing either the plasma membrane or all membranes. We found that a 30-second exposure of PFA-fixed BMMs to digitonin permeabilized the plasma membrane while leaving TXR–Dex-labeled macropinosomes intact (Fig. 2A), whereas Triton X-100 permeabilized both the plasma membrane and macropinosomes (supplementary material Movie 4). Staining of CSF-1-starved BMMs showed that in the absence of either permeabilization, the extracellular epitope of the CSF-1R could be seen on the plasma membrane and that digitonin permeabilization was required for staining of the cytosolic

Journal of Cell Science (2014) 127, 5228–5239 doi:10.1242/jcs.154393

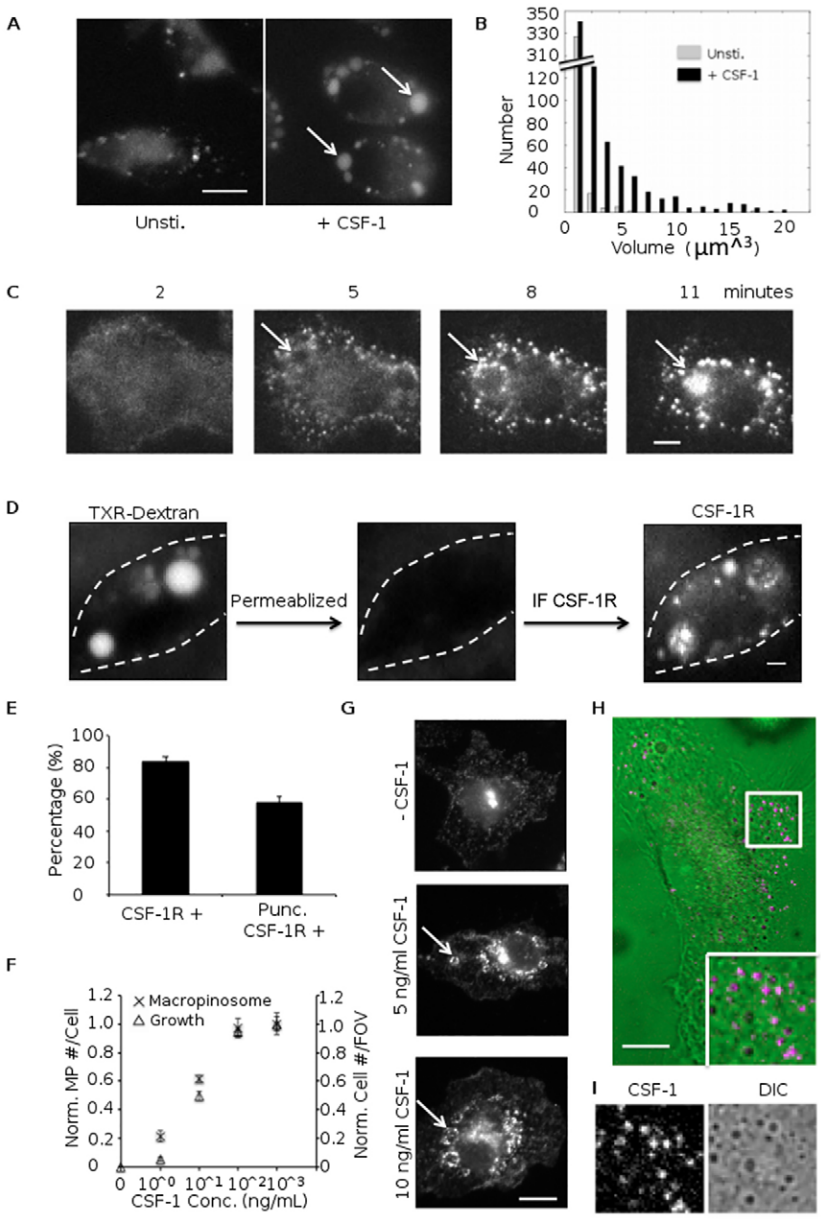

Fig. 1. Internalized CSF-1 and the CSF-1R are delivered to the lumen of newly formed macropinosomes at CSF-1 concentrations that stimulate BMM proliferation. (A) Macropinocytosis was stimulated by a 5-minute exposure to CSF-1, as observed by the uptake of Texas-Red–dextran (TXR–Dex, 70 kDa). White arrows indicate macropinosomes, which contain TXR–Dex and appear as large round objects. Unsti., unstimulated. Scale bar: 5 μm. (B) A histogram of the volume of TXR–Dex-labeled macropinosomes induced by CSF-1. $n=50$ cells; data are representative of three experiments. (C) Imaging of BMMs exposed to a 1-minute pulse of TXR–CSF-1 showed that TXR–CSF-1 was internalized in small endosomes that underwent fusion to produce brighter slightly larger endosomes (punctate structures at 2 and 5 minutes). Macropinosomes were visible as displaced cytoplasm (5 minutes, arrow) to which endosomes containing TXR–CSF-1 were trafficked (8 min, arrow). As the macropinosome matured, TXR–CSF-1 was delivered into the lumen (11 min, arrow). Scale bar: 2 μm. (D) The CSF-1R localized to punctate structures within macropinosomes after a 15-minute exposure to CSF-1. Macropinosomes marked by TXR–Dex (70 kDa) were fixed and permeabilized, causing the dextran to leak out. Samples were subsequently stained for the CSF-1R. The dashed line indicates the outline of the cell. IF, immunofluorescence. Scale bar: 1 μm. (E) CSF-1R localization to macropinosomes after a 15-minute exposure to CSF-1 was quantified from the data shown in D as the percentage of TXR–Dex-positive macropinosomes per cell that are CSF-1R positive (CSF-1R +) and contain a punctate distribution of CSF-1R (punc. CSF-1R). $n=50$ cells; data are representative of three experiments and show the mean±s.e.m. (F) BMM growth and macropinocytosis were measured as a function of constant CSF-1 concentrations (conc.) after 7 days in culture. Norm. MP, normalized macropinosome; FOV, field of view. Data are representative of three experiments and show the mean±s.e.m. (G) Immunofluorescence against the CSF-1R in BMMs exposed to 5 and 10 ng/ml CSF-1 for 15 minutes. Arrows indicate macropinosomes. Scale bar: 5 μm. (H) TXR–CSF-1 localized to macropinosomes in human monocyte-derived macrophages following an 8-minute exposure to TXR–CSF-1. Macropinosomes are shown in green (DIC) and TXR-CSF-1 is in magenta. Scale bar: 10 μm. (I) Zoom of the indicated region in H.

epitope (Fig. 2B). Under all conditions, the antibody recognizing the cytosolic tail also gave a weak perinuclear staining pattern that we attribute to a non-specific reaction because this fraction could not be stained by the antibody recognizing the extracellular epitope. After 5 minutes of CSF-1 exposure, only the antibody recognizing the CSF-1R cytosolic epitope could be detected on early endosomes during digitonin permeabilization, consistent with the receptor residing in early endosomes (Fig. 2C). Following permeabilization with Triton X-100, both antibodies stained the CSF-1R (Fig. 2C), indicating that the receptor was intact, but that the extracellular epitope was protected by the early endosomal membrane during digitonin permeabilization. Following 15 minutes of CSF-1, the CSF-1R could only be localized to a few small puncta with either antibody during plasma membrane permeabilization, indicating lipid membranes protected both epitopes. Total membrane permeabilization with Triton X-100 allowed both epitopes to be stained and revealed a strong colocalization on large macropinosome structures matching those observed in our sequential staining experiments (Fig. 2D; Fig. 1D; supplementary material Fig. S3). These results provide strong evidence that the CSF-1R is transported into the lumen of macropinosomes, likely by the conversion of the macropinosome into an MVB.

The CSF-1R is internalized by small vesicle endocytosis with only minor uptake by macropinocytosis

To determine whether macropinocytosis mediates internalization of the CSF-1R by bulk internalization of plasma membrane, we found an unrelated chemokine, CXCL-12, that stimulated macropinocytosis to the same level as CSF-1 (Fig. 3B). Following CXCL-12 exposure, the CSF-1R was rarely localized to macropinosomes and, when observed, was only present at densities less than those found on the plasma membrane (Fig. 3A,C). This result was easily discernable from BMMs exposed to CSF-1, which showed a dramatic redistribution of the CSF-1R to macropinosomes (Fig. 3A). Furthermore,

Journal of Cell Science (2014) 127, 5228–5239 doi:10.1242/jcs.154393

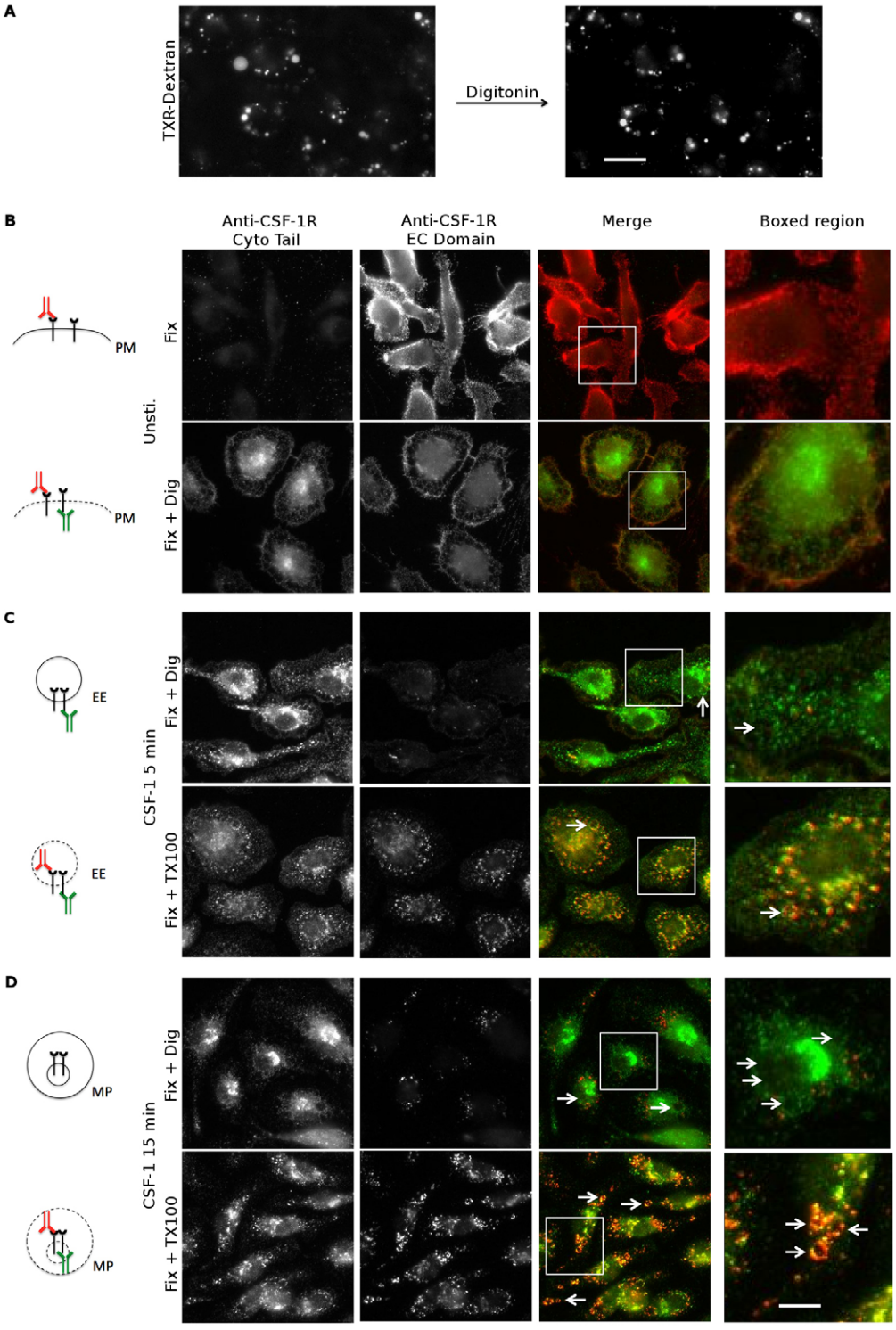

Fig. 2. Activated CSF-1R is sequestered within the lumen of macropinosomes. (A) Images of CSF-1-stimulated BMMs containing TXR–Dex-labeled macropinosomes before and after selective membrane permeabilization with digitonin. Scale bar: 10 µm. (B–D) BMMs were co-stained with CSF-1R antibodies recognizing either the cytosolic tail (Cyto tail, green) or extracellular domain (EC domain, red) to determine to the topology of trafficking CSF-1R. (B) Resting (unstimulated, Unsti.) BMMs were either fixed or fixed and permeabilized with digitonin (dig). Note the absence of cytoplasmic tail staining in the unpermeabilized cells. Following digitonin treatment, both the extracellular and intracellular epitopes of the CSF-1R could be stained. PM, plasma membrane. (C) Images of digitonin- and Triton X-100 (TX100)-permeabilized BMMs 5 minutes after exposure to CSF-1. CSF-1R was internalized and only the cytosolic tail stained following permeabilization with digitonin, whereas cells that underwent total membrane permeabilization with Triton X-100 showed staining for both the cytosolic tail and the extracellular domain, suggesting the extracellular domain was protected by the membrane of the early endosome (EE). (D) Digitonin- and Triton-X-100-permeabilized BMMs 15 minutes after exposure to CSF-1. Neither epitope was accessible with digitonin permeabilization, indicating full enclosure of the CSF-1R in macropinosomes (MP). Triton X-100 exposed both epitopes within macropinosomes. Arrows indicate receptor clustering within macropinosomes. Boxes in the merged images indicated regions that are enlarged to the right. Scale bar: 3.3 µm.

CXCL-12-induced macropinocytosis did not reduce the cell surface CSF-1R density, other than what could be attributed to cell spreading, whereas ligated CSF-1R was rapidly cleared from the cell surface (Fig. 3D,E). Taken together, these results indicate that macropinocytosis and the bulk internalization of plasma membrane associated with this process is an inefficient endocytic route for resting CSF-1R.

To test the selectivity of this pathway, we stimulated cells with both CSF-1 and CXCL12 and assessed the localization of the CSF-1R and CXCR4 (the CXCL12 receptor). The CSF-1R rapidly accumulated in macropinosomes; however, CXCR4 did not redistribute to macropinosomes at levels above those seen on the plasma membrane (Fig. 3F), indicating that this process was selective for the CSF-1R. Furthermore, we imaged the internalization of fluorescent transferrin as a proxy for the transferrin receptor during exposure of cells to CSF-1. Consistent with the previous observations (Racoosin and Swanson, 1992), macropinocytosis resulted in trace amounts of transferrin uptake,

Journal of Cell Science (2014) 127, 5228–5239 doi:10.1242/jcs.154393

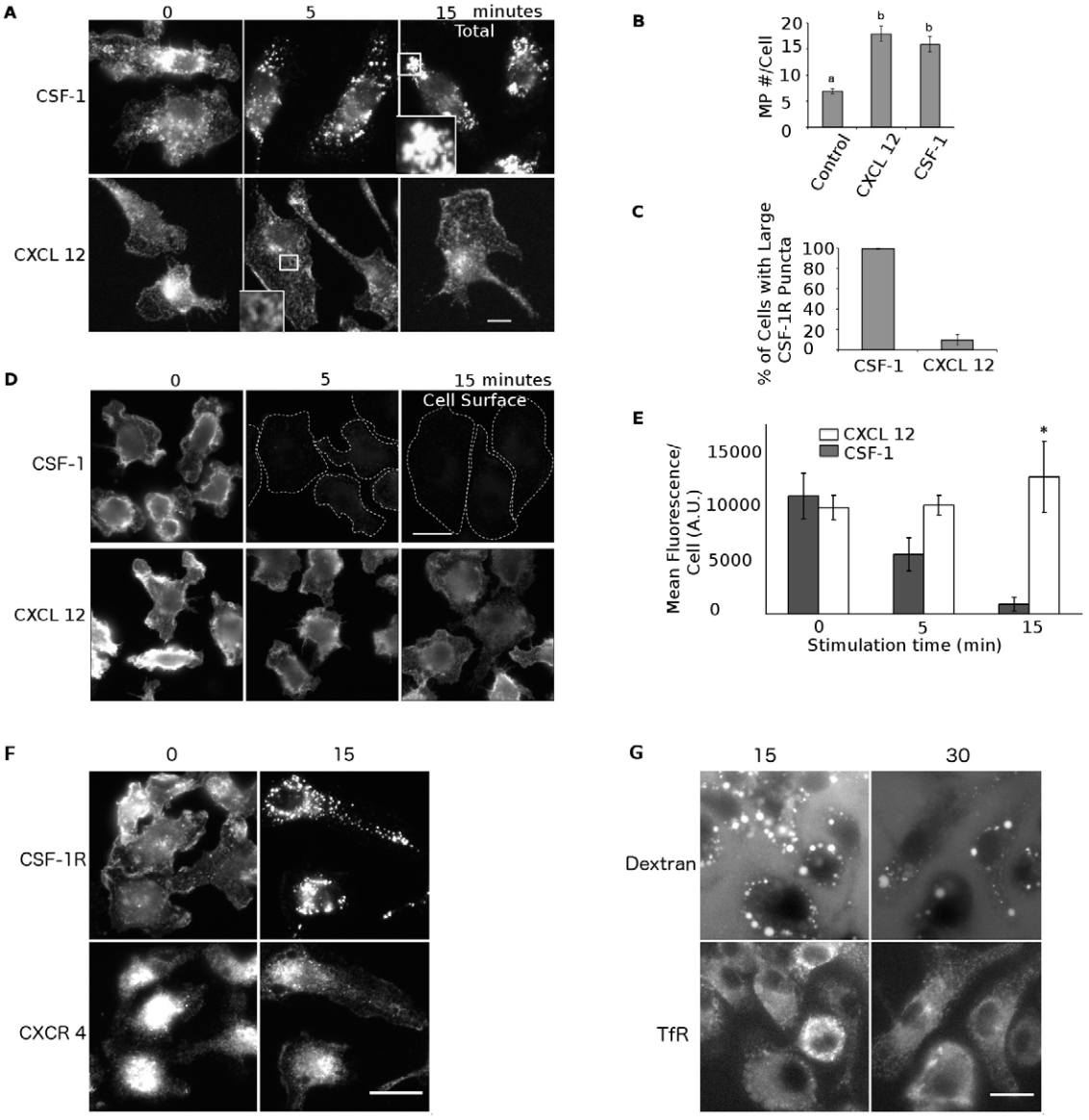

Fig. 3. CSF-1R internalization is mediated predominantly by clathrin-sensitive small vesicle endocytosis with macropinosomes playing a minor role. (A) BMMs were stimulated with CXCL12 or CSF-1 and stained for total CSF-1R following fixation and Triton-X-100-mediated permeabilization. Note the lack of clustering and internalization of CSF-1R when stimulating with CXCL12. Boxed areas are shown at higher magnification in the lower left corner. Scale bar: 5 μm. (B) Quantification of macropinosomes (MP) per cell from A. Data show the mean±s.e.m. (n=30 cells). Bars not connected by the same letter are significantly different (P<0.05, ANOVA followed by Tukey HSD post hoc analysis. (C) Quantification of the localization of CSF-1R to macropinosomes after treatment with CSF-1 or CXCL12 for 15 minutes. Data show the mean±s.e.m. (n=240 cells across three experiments); P<0.001 (Student's t-test). (D) Cell surface staining of the CSF-1R after stimulation with CSF-1 or CXCL12 in BMMs. Dashed white lines show cell outlines. Scale bar: 10 μm. (E) Quantification of the CSF-1R cell surface fluorescence intensity during CXCL12 and CSF-1 treatment. A.U., arbitrary units. Data show the mean±s.e.m. (n>50 cells from two experiments); *P<0.05 (two-way ANOVA followed by Sidak's multiple comparison test). (F) BMMs were stained for total CSF-1R and CXCR4 before and after exposure to CSF-1 and CXCL12. CSF-1R was selectively transported to macropinosomes, whereas CXCR4 was not. Scale bar: 10 μm. (G) BMMs were treated with CSF-1 (3 minutes) and chased for the times indicated before visualizing the presence of Oregon-Green–transferrin (TfR) and 10,000 Da TXR–Dex. Scale bar: 10 μm.

which was subsequently depleted from the macropinosomes, indicating that the transferrin receptor did not accumulate in macropinosomes as was true for the CSF-1R (Fig. 3G). Taken together, these results indicate that the CSF-1R is selectively targeted to the macropinosome when ligated.

Given the small size of the endocytic vesicles carrying CSF-1 (Fig. 1) and the established role of CME in RTK endocytosis (Sorkin and Goh, 2009), we speculated that CME was the predominant mechanism for CSF-1R endocytosis. Indeed, RNA interference (RNAi)-mediated knockdown of clathrin heavy chain 1 (CHC) impaired CSF-1R endocytosis as measured by clearance of CSF-1R from the cell surface (Fig. 4A,B). Near complete knockdown of CHC took 6 days and two rounds of RNAi transfection, during which the cell surface density of the CSF-1R dropped, possibly owing to either failure of transport of the CSF-1R to the cell surface or transcriptional repression. To overcome this limitation, we compared the drop in the CSF-1R cell surface density with the arrest in transferrin uptake during clathrin

Journal of Cell Science (2014) 127, 5228–5239 doi:10.1242/jcs.154393

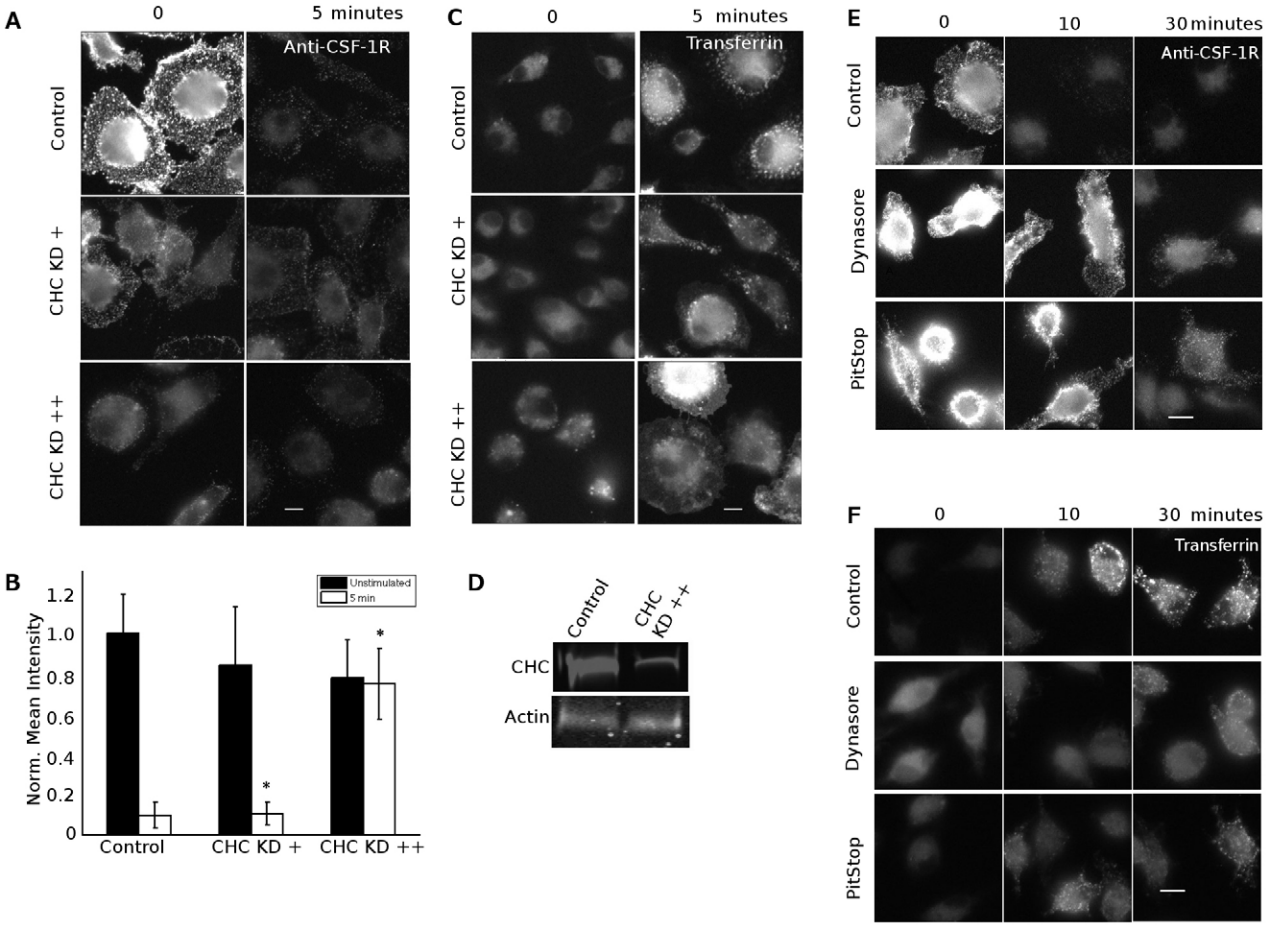

Fig. 4. Endocytosis of the CSF-1R is sensitive to clathrin inhibition. (A) Surface staining of CSF-1R in resting and CSF-1-stimulated BMMs that were transfected once (CHC KD+) or twice (CHC KD++) with RNAi oligos specific to CHC. See Materials and Methods. Scale bar: 5 μm. (B) Quantification of CSF-1R surface staining on resting and CHC-knockdown (KD) BMMs. Norm., normalized. Data show the mean±s.d. (n=25 cells per condition); *P<0.05 (two-way ANOVA followed by Sidak's multiple comparison test; no difference for CHC KD++). (C) Transferrin uptake in CHC knockdown BMMs. Transferrin was used at 10 μg/ml. Scale bar: 5 μm. (D) Western blot showing reduction of CHC protein levels in CHC KD++ BMM cells. (E) Surface staining CSF1-R on BMMs treated with the CME inhibitory drugs dynasore or PitStop2 and exposed to CSF-1 for the indicated times. Scale bar: 5 μm. (F) Images of fluorescent transferrin uptake in BMMs treated with dynasore or PitStop2 as in C. Scale bar: 5 μm.

knockdown. In control BMMs and those exposed to CHC RNAi for 3 days, CSF-1R and transferrin internalization were unaffected (Fig. 4A–C). However, following 6 days of RNAi, CHC was substantially depleted (Fig. 4D), CSF-1R internalization halted (Fig. 4A,B) and transferrin accumulated on the cell surface (Fig. 4C). Consistent with these results, treatment with the dynamin inhibitor dynasore (Macia et al., 2006) and the clathrin inhibitor PitStop2 (von Kleist et al., 2011) impaired clearance of the CSF-1R from the cell surface as well as transferrin uptake (Fig. 4E,F). The correlation of impaired CSF-1R internalization with impaired transferrin internalization under both inhibitor and CHC RNAi is consistent with CME as the route of entry. However, impaired delivery of the CSF-1R to the cell surface during CHC knockdown and possible inhibitor specificity issues (Dutta et al., 2012; Park et al., 2013; Willox et al., 2014) suggest that other small vesicle endocytic routes, such as caveolin-mediated endocytosis might be possible. Nonetheless, small vesicle endocytosis was the predominant route of CSF-1R internalization. This observation was corroborated by the fact that inhibition of macropinocytosis by disruption of the actin cytoskeleton had little or no effect on clearance of activated CSF-1R from the cell (Fig. 6D).

Macropinosomes are Rab5 positive during CSF-1R arrival and become Rab7 positive during transport of the CSF-1R into their lumen

To stage the transport of CSF-1R to nascent macropinosomes, we imaged the arrival of TXR–CSF-1 relative to mCit–Rab5a or YFP–Rab7. Upon exposure of BMMs to CSF-1R, pronounced membrane ruffling and the formation of mCit–Rab5a-positive macropinosomes were observed (supplementary material Movie 5). Other than macropinosomes, few if any pre-existing micrometer-scale Rab5-positive structures were observed in these cells, indicating that the low level expression of mCit–Rab5a resulting from retroviral transduction did not drive the formation of enlarged endosomes (supplementary material Movie 5). Following internalization (~2 min), small TXR–CSF-1-containing endosomes acquired mCit–Rab5a, during which time they began to fuse into early endosomes, as seen by their increase in brightness and size (Fig. 5A,B; supplementary material Movie 5). Colocalization between TXR–CSF-1 and mCit–Rab5a was maximal around 5 minutes after addition of TXR–CSF-1 (Fig. 5C). At this point, TXR–CSF-1-containing endosomes arrived at macropinosomes decorated with mCit–Rab5a (Fig. 5D, 6.3 minutes). In the majority of cases, TXR–CSF-1-containing

Journal of Cell Science (2014) 127, 5228–5239 doi:10.1242/jcs.154393

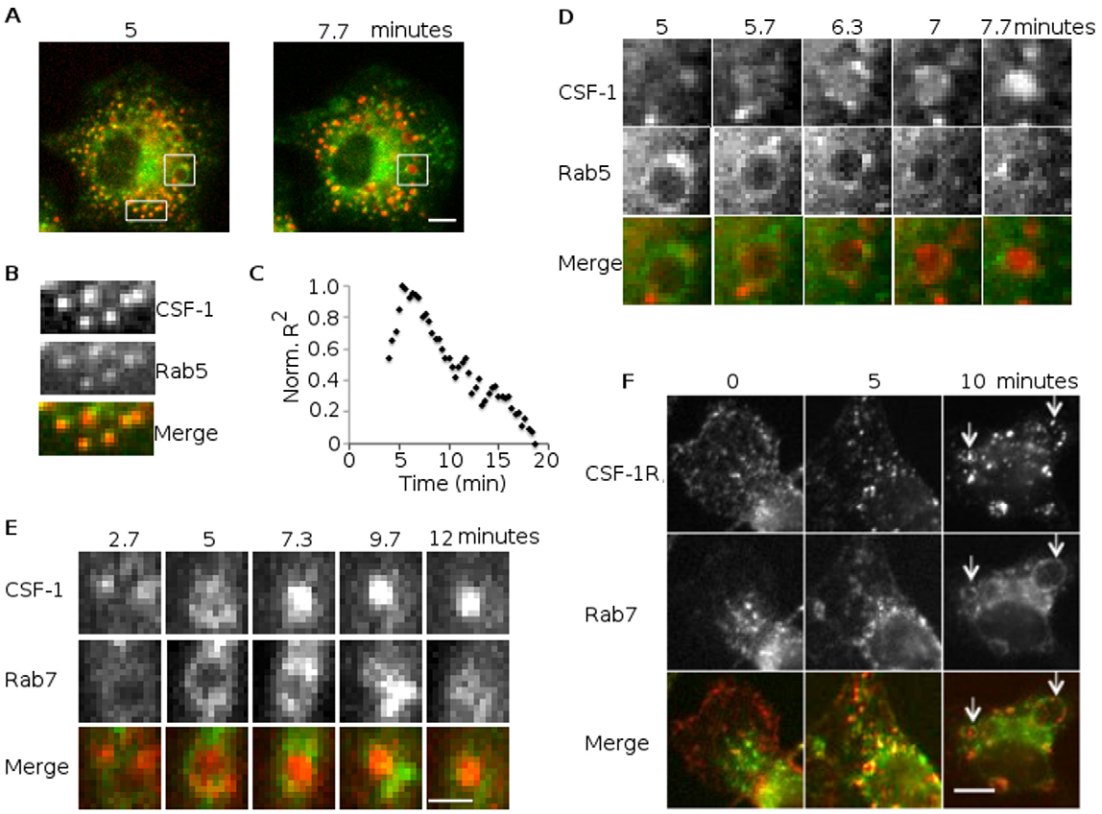

Fig. 5. Macropinosomes are Rab5 positive during CSF-1 endosome delivery and transition to Rab7 positive during CSF-1 delivery to their lumen. (A) Movies of BMMs expressing mCit–Rab5a (green) and exposed to TXR–CSF-1 (red) for 1 minute were recorded (supplementary material Movie 5). Images shown here highlight the trafficking of TXR–CSF-1 in endosomes (5 minutes) and their trafficking to macropinosomes (7.7 minutes). Scale bar: 5 μm. (B) Zoom of the rectangular region in A (5 minutes), showing colocalization of TRX–CSF-1 (red) and mCit–Rab5a (yellow). (C) Normalized (Norm.) Pearson correlation coefficient between mCit–Rab5a and TXR–CSF-1 fluorescence intensities. The peak correlation occurs around the time at which TXR–CSF-1 was delivered to the macropinosomes (~6 minutes, average of ten cells). (D) A zoom of the square boxed region in A shows mCit–Rab5a-negative TXR–CSF-1-positive endosomes fused with mCit–Rab5a-positive macropinosomes. (E) BMMs transduced with YFP–Rab7 (green) and exposed to TXR–CSF-1 for 1 minute were imaged. Frames at the indicated times show macropinosomes acquiring YFP–Rab7 when TXR–CSF-1 was transported into their lumen. Scale bar: 2 μm. (F) BMMs were stained for endogenous Rab7 (green) and total CSF-1R (red) after exposure to 100 ng/ml CSF-1 for the times indicated. Arrows highlight Rab7-positive macropinosomes containing TXR–CSF-1. Scale bar: 5 μm.

endosomes lost mCit–Rab5a prior to their arrival at Rab5-positive macropinosomes (Fig. 5D). We point out, however, that movement of macropinosomes and TXR–CSF-1-containing endosomes towards the Rab5a-rich perinuclear region precluded a definitive conclusion on the timing of endosome–macropinosome fusion and Rab5 loss. By 8 minutes, the TXR–CSF-1 endosomes fused with macropinosomes (Fig. 5D). These macropinosomes then transitioned from mCit–Rab5a positive to YFP–Rab7 positive, and TXR–CSF-1 was delivered to the macropinosome lumen (Fig. 5E,F). Consistent with our CSF-1R staining (Fig. 1D; Fig. 2), we interpret the translocation of TXR–CSF-1 (Fig. 5D,E) as a translocation of the CSF-1R to the lumen during macropinosome maturation into a late endosome.

Macropinosomes mediate CSF-1R degradation but not internalization

Delivery of CSF-1 and the CSF-1R to the lumen of macropinosomes suggested that macropinosomes are the site of CSF-1R degradation. Following a 3-minute pulse of 100 ng/ml CSF-1, the CSF-1R was internalized and degraded without recycling to the cell surface (Chen and Lin, 1984; supplementary material Fig. S4). During this time, CSF-1 and the CSF-1R trafficked to macropinosomes (Fig. 1C,D; supplementary material Movies 2, 3). These macropinosomes shrank and underwent fusion with each other as they matured (supplementary material Movies 1, 2), reducing the number and size of macropinosomes in each cell. During this time, CSF-1R remained localized to the shrinking macropinosomes and was completely degraded by 60 minutes (Fig. 6A).

To determine whether macropinosomes mediate the degradation of the CSF-1R, we used a number of previously described inhibitors of macropinocytosis. These included amiloride and its more potent analog 5-(N-ethyl-N-isopropyl)amiloride (EIPA), compound C and expression of dominant-negative Rab5 and Rac1. Although all of these approaches reduced macropinocytosis to about a quarter of its normal levels, none of them eliminated it, and many of these approaches altered receptor traffic and membrane organization (data not shown). We concluded that the best way to block macropinocytosis was to acutely disrupt the actin cytoskeleton using the actin depolymerizing drug latrunculin B and the myosin IIa inhibitor blebbistatin in combination with the F-actin stabilizer and fragmenter jasplakinolide (Mercer et al., 2010). Acute exposure to latrunculin B (5 min) or the blebbistatin/jasplakinolide combination (15 min) completely blocked macropinocytosis as assayed by TXR–Dex uptake (Fig. 6B,C).

Journal of Cell Science (2014) 127, 5228–5239 doi:10.1242/jcs.154393

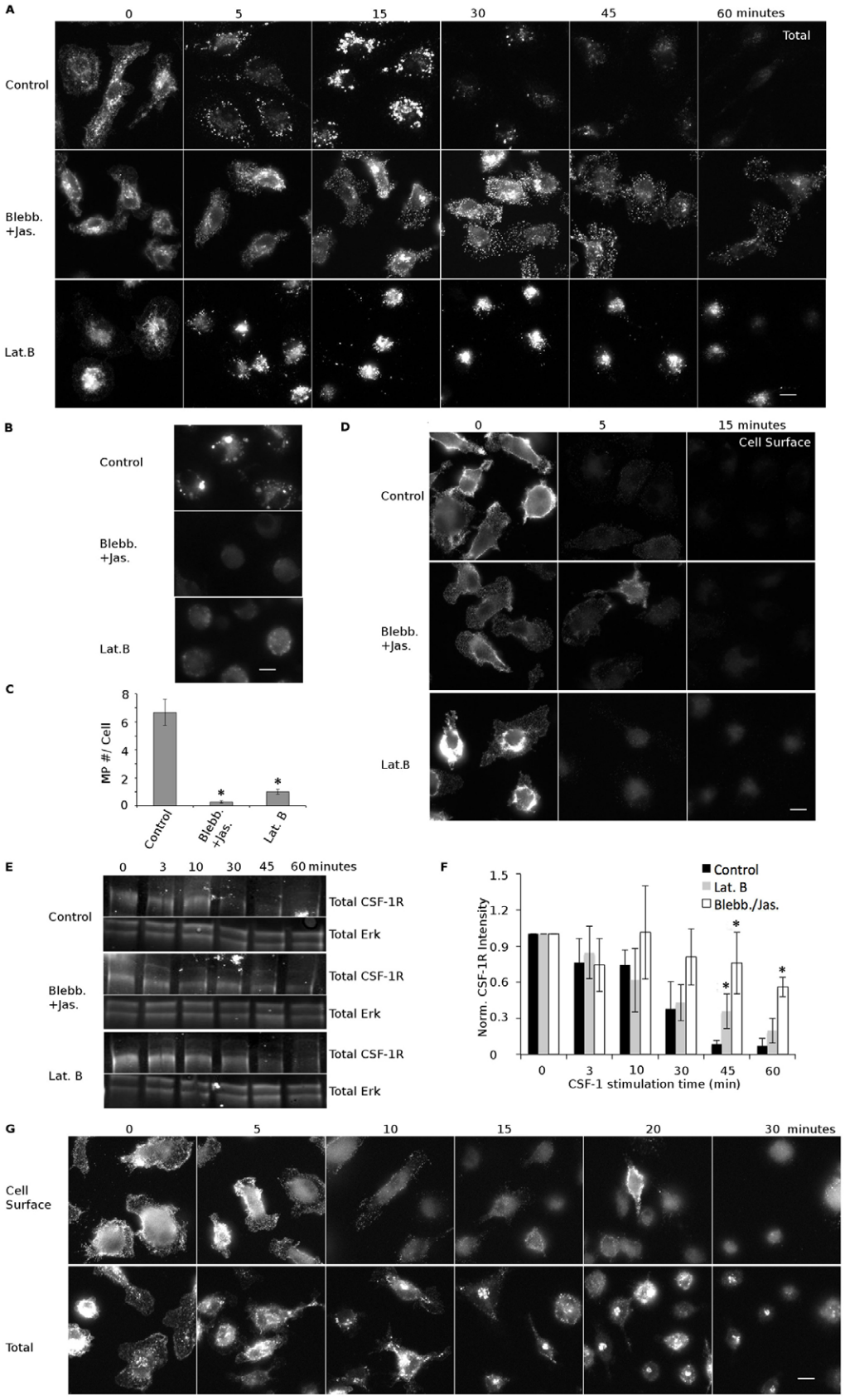

Fig. 6. Macropinocytosis is required for efficient receptor degradation. BMMs were left untreated or were treated with blebbistatin (Blebb., 75 μM, 10-minute pretreatment) plus jasplakinolide (jas., 1 μM, 5-minute pretreatment) or with latrunculin B (Lat.B, 0.5 μM, 5 minutes) and then exposed to CSF-1 for the indicated times. (A) Images of total CSF-1R show that the receptor was redistributed to small endosomes (5 minutes) and then trafficked to macropinosomes (15 minutes) that condensed and underwent fusion (30 minutes and 45 minutes) until the CSF-1R was no longer detectable (60 minutes). Blocking macropinocytosis with blebbistatin plus jasplakinolide or with latrunculin B slowed CSF-1R degradation. Scale bar: 5 μm. (B) Treatment with blebbistatin plus jasplakinolide or with latrunculin B blocked CSF-1-induced macropinocytosis as seen by the loss of TXR–Dex uptake. Scale bar: 10 μm. (C) Quantification of macropinosome (MP) number from B. Data show the mean±s.e.m. (n=40 cells, three experiments); *P<0.001 between control and treatments (Student's t-test). (D) Cell surface staining of CSF-1R indicates that blocking macropinocytosis does not affect receptor internalization in latrunculin-B-treated cells and causes only a small delay in blebbistatin plus jasplakinolide-treated cells. Scale bar: 10 μm. (E) Western blotting for the CSF-1R demonstrated that blocking macropinocytosis slows down CSF-1R degradation. (F) Quantification of western blots. Norm., normalized. Data show the mean±s.d. (three independent experiments); *P<0.05 between control and treatments (Student's t-test). (G) EIPA triggers receptor internalization and degradation. Cell surface CSF-1R disappeared quickly in EIPA-treated cells (40 μM, durations of pretreatment are indicated). Total receptor immunofluorescent staining demonstrated that receptor was internalized and degraded in EIPA-treated cells. Scale bar: 5 μm.

Importantly, these treatments had little or no impact on CSF-1R endocytosis as assayed by cell surface staining for the CSF-1R (Fig. 6D). Actin-based disruption of macropinocytosis slowed the degradation of the CSF-1R. By using immunofluorescence, we observed that small CSF-1R-containing vesicles persisted in the actin-disrupted BMMs for over an hour, whereas most of the

Journal of Cell Science (2014) 127, 5228–5239 doi:10.1242/jcs.154393

CSF-1R was destroyed between 15 and 30 minutes in unperturbed macrophages (Fig. 6A). Immunoblotting against the CSF-1R confirmed the immunofluorescence results indicating that a blockade of macropinocytosis by actin disruption slowed CSF-1R degradation (Fig. 6E,F). These results indicate that macropinosomes are likely to accelerate the degradation of the CSF-1R, but are not required for this process (Fig. 6). Furthermore, they point towards the need for more selective methods of inhibiting macropinocytosis, as acute actin disruption could have pleiotropic effects on membrane traffic that make it impossible to clearly delineate the degree to which the macropinosome accelerates CSF-1R degradation.

In our search for macropinosome-blocking drugs, we were surprised to find that the commonly used amiloride-based inhibitor EIPA triggered rapid internalization and degradation of the CSF-1R (Fig. 6G). Recently, this inhibitor has been used to study macropinocytosis in the context of the cancer cell growth (Commisso et al., 2013). In the macrophage context, however, reduction in macropinocytosis by EIPA might be due to loss of CSF-1R signaling rather than a direct action on the proposed Na^+/H^+ exchanger and alteration of inner leaflet pH (Koivusalo et al., 2010).

DISCUSSION

Our data define a model in which the CSF-1R is internalized by small vesicle endocytosis and is then transported to nascent macropinosomes and degraded (Fig. 7). Initially, we speculated that the large surface area of plasma membrane consumed during CSF-1-stimulated macropinocytosis would be an efficient route for CSF-1R internalization. This idea was supported by the previous reports that CSF-1–CSF-1R localizes to large endocytic structures (Boocock et al., 1989; Murray et al., 2000) and reports of Rac, PI3K and Ras signaling to CSF-1-stimulated macropinosomes (Welliver et al., 2011; Yoshida et al., 2009). However, our results showed only traces of CSF-1 or CSF-1R on forming macropinosomes. Rather, we found that the CSF-1 and CSF-1R accumulated rapidly at small endocytic sites that were sensitive to disruption of clathrin and dynamin (Fig. 3). Furthermore, inhibition of the actin cytoskeleton blocked macropinocytosis but had little effect on CSF-1R internalization. Thus, the CSF-1R must stimulate macropinocytosis through signaling by, for example, PI3K, Ras and PLC (Amyere et al., 2000; Maekawa et al., 2014; Veltman et al., 2014), which can diffuse away from the CSF-1R during its accumulation at sites of small vesicle endocytosis (Fig. 6). These diffuse signals must remotely self-organize at sites of macropinocytosis through the creation of local diffusion barriers (Welliver et al., 2011; Yoshida et al., 2009).

Our data suggest a new role for macropinosomes in RTK signaling. Multiple RTKs have been observed within macropinosomes (Trk, PDGFR) (Philippidou et al., 2011; Schmees et al., 2012) following exposure to growth factors. For macropinocytosis to mediate the endocytosis of RTKs, internalization of bulk plasma membrane would need to compete with CME or other small vesicle endocytosis of RTKs. Our data indicates that small vesicle endocytosis of the CSF-1R is much faster than macropinocytosis. Thus, our data are consistent with a model in which macropinosomes produced in response to RTK signaling mediate receptor sequestration and degradation but not internalization. Trafficking of RTKs to 500–1000-nm diameter vesicles has been widely reported in the literature; however, these compartments are often thought to arise from the fusion of small endosomes carrying the receptors to create late endosomes and MVBs (Boocock et al., 1989; Raiborg and Stenmark, 2009).

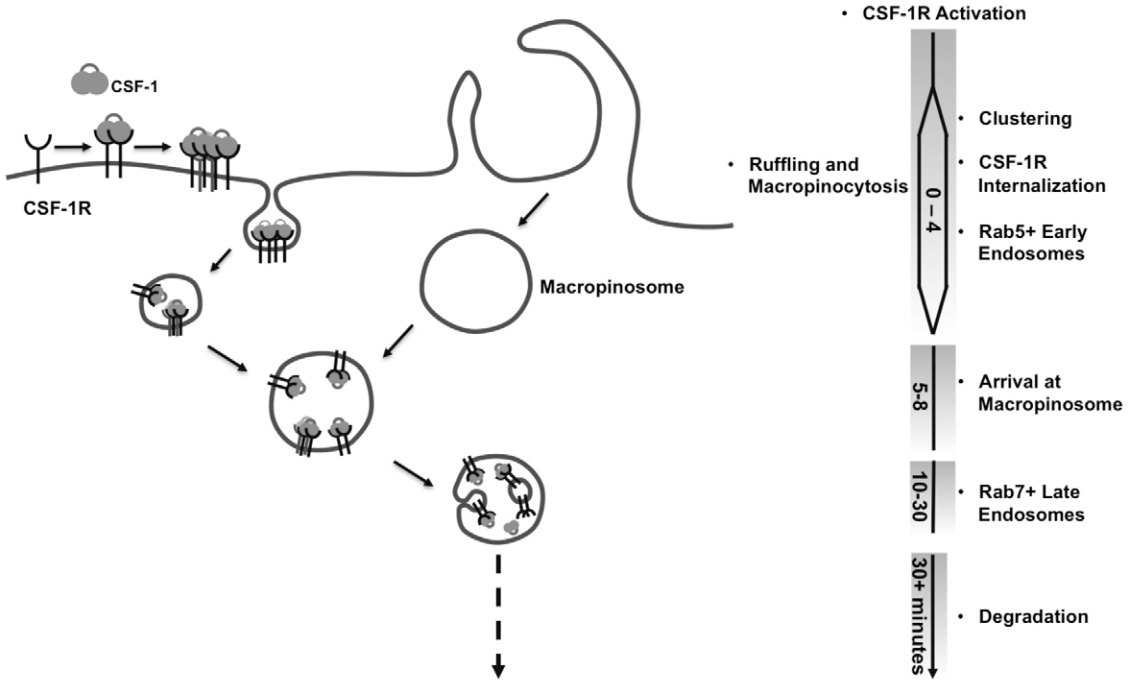

Fig. 7. Model for CSF-1R endocytosis and trafficking to macropinosomes. Ligated CSF-1R stimulates the production of macropinosomes as it is internalized by small vesicle endocytosis. CME endosomes undergo homotypic fusion before trafficking to Rab5-positive macropinosomes. Macropinosomes mature into Rab7-positive late endosomes, whereupon the receptor is delivered to their lumen. The CSF-1R is finally degraded ~45 min after expose to CSF-1. This model indicates that macropinosomes serve as a site of MVB biogenesis.

Journal of Cell Science (2014) 127, 5228–5239 doi:10.1242/jcs.154393

Although a number of trafficking mechanisms might exist for different cell types, in primary macrophages at physiological ligand concentrations, macropinocytosis appears to be the primary mechanism leading to the formation of large late endosomes to which CSF-1R selectively traffics. The live-cell imaging of fluorescent CSF-1 traffic allowed us to capture this rapid internalization and transport to the macropinosome. Careful analysis of the trafficking of other RTKs will be needed to distinguish the endocytic roles and late endosome roles of macropinosomes from the conventional models.

What targets CSF-1R vesicles to the macropinosome? Our data indicate that homotypic fusion of small Rab5-positive vesicles (Rink et al., 2005; Sorkin and Goh, 2009) occurs prior to the delivery of the CSF-1R to the macropinosome (Fig. 3D). It is possible that fusion of these Rab5-positive early endosomes with Rab5-positive macropinosomes contributes to delivery. However, within our data, many of the early endosomes arriving at the macropinosome appeared to be Rab5 negative, suggesting that another mechanism might target CSF-1R-containing endosomes to the macropinosome. Additional experiments that manipulate Rabs and other trafficking machinery will be needed to define these mechanisms.

Macropinosomes degrade the CSF-1R in their lumen, indicating that they are precursors to MVBs. During the acquisition of Rab7, the CSF-1R was transported into the lumen of the macropinosome (Figs 2, 5) and degraded by ~30 minutes post-exposure to CSF-1 (Fig. 6). These results are consistent with the data, obtained by using electron microscopy, that in peritoneal macrophages, I^{125}-CSF-1 localizes to large vacuoles that contain debris, some of which resembles lumenal vesicles (Chen and Lin, 1984), and the observation that large vacuoles containing lumenal vesicles were observed by electron microscopy in RAW 264.7 macrophages allowed to internalize horseradish peroxidase by fluid-phase endocytosis and macropinocytosis (Braun et al., 2004). Taken together, these data indicate that macropinosomes can serve as sites for lumenal budding and might be MVB precursors. Electron microscopy studies will be needed to determine the prevalence of MVB formation and additional molecular biology will be needed to determine the machinery responsible for transporting the receptor into the lumen. The robustness of this process (supplementary material Fig. S3) indicates that macropinosomes contribute to CSF-1R signal termination by accelerating the sequestration of the cytoplasmic tail of CSF-1R into macropinosomes (Fig. 2). Furthermore, the observation of this mechanism in both mouse and human macrophages underscores the relevance of this mechanism for controlling macrophage function.

Macropinosomes might couple signal amplification with signal termination. Although CSF-1R signaling originates at the plasma membrane, recent evidence indicates that sustained signaling from internalized CSF-1R through the MAPK–Erk pathway mediates transcriptional changes associated with growth (Huynh et al., 2012). CSF-1R trafficking to the macropinosome is consistent with this observation and with the proposed roles of macropinocytosis in amplifying signal from other RTKs such as the PDGFR and Trk receptors (Philippidou et al., 2011; Schmees et al., 2012). Thus, the macropinosome might be a trafficking destination for the CSF-1R as a possible mechanism for amplifying signaling while also serving as their signal terminators through delivery to the macropinosome lumen.

Traffic of the CSF-1R to the macropinosome might link CSF-1 signaling to nutrient uptake. Specifically, we observed that macrophage proliferation and macropinocytosis are tightly coupled over the range of CSF-1 concentrations that support macrophage growth (Fig. 1). Recent work has shown that in Ras(V12)-transformed cancer cells, macropinocytosis of serum proteins provides an amino acid supply *in vitro* and *in vivo* (Commisso et al., 2013). Thus, it is likely that CSF-1 signaling drives macropinocytosis for nutrient uptake in macrophages, which have evolved to be efficient at the uptake and degradation of extracellular protein. Trafficking of the CSF-1R to the macropinosome might couple CSF-1R signaling with nutrient sensing (Laplante and Sabatini, 2012).

MATERIALS AND METHODS

Reagents

Primary antibodies were acquired that recognized an extracellular epitope or intracellular domain for the CSF-1R (clone AFS98, eBioscience; SC692, Santa Cruz Biotechnology), CXCR4 (SC9046, Santa Cruz Biotechnology), Rab7 (clone D95F2, Cell Signaling Technology) and the clathrin heavy chain (CHC) (clone sc-12734, Santa Cruz Biotechnology). Secondary antibodies were conjugated to Alexa Fluor 488 (Life Technologies), Dylight 690, Dylight 780 or Dylight 594 (Thermo Fisher Scientific). CSF-1 was labeled using the succinimidyl ester of Texas Red-X (TXR; catalog number T-6134; Life Technologies) or Dylight 594 (product number 46412, Thermo Fisher Scientific). Macropinosome blocking experiments used several drugs, including latrunculin B (Santa Cruz Biotechnology), 5-(N-ethyl-N-isopropyl)amiloride (EIPA, Sigma), jasplakinolide and blebbistatin (Enzo Life Science). Macropinosomes were specifically labeled using TXR–Dex (70,000 Da, Life Technologies) or Lucifer Yellow (LY, Sigma). Blockade of endocytosis used dynasore (Sigma) or PitStop2 (Abcam), as described previously (Macia et al., 2006; von Kleist et al., 2011). Alternative stimulation of macropinocytosis used the recombinant chemokine CXCL12 (also known as SDF-1a, PeproTech). Mammalian-expressed human recombinant CSF-1 (Biolegend) was used in hMDM culture. Dulbecco's Modified Eagle Medium (DMEM, Hyclone) and fetal bovine serum (Hyclone) were used for cell culture. Ni-NTA affinity resin (Qiagen) was used in CSF-1 purification. Digitonin and Triton X-100 (Sigma) were used to permeabilize cells.

Recombinant CSF-1 purification, labeling and functional assay

Recombinant CSF-1 (N-terminal 151 amino acids) was purified from *Escherichia coli*. A sequence for the N-terminal 453 nucleotides of CSF-1 cDNA (Biosystem) was amplified and cloned into the pQE31 plasmid between the restriction sites for *Bam*HI and *Hind*III using standard digestion and ligation to enable expression of 6×His–CSF-1. Protein expression was carried out in BL21(DE3) *E. coli* under induction by isopropyl β-D-1-thiogalactopyranoside (IPTG). CSF-1 inclusion bodies were solubilized in urea buffer [8 M urea, 100 mM NaH_2PO_4, 10 mM Tris-HCl pH 8.0, 10 mM dithiothreitol (DTT)] overnight at room temperature, and His–CSF-1 was purified by affinity chromatography according to the manufacturer's instructions. Purified monomeric His–CSF-1 was refolded by dilution into glycine buffer (50 mM glycine pH 9.0) at a concentration of 0.3 mg/ml. Refolded CSF-1 dimers were separated from monomers by gel-filtration chromatography (HiPrep Sephacryl S-100 HR, GE-Healthcare; supplementary material Fig. S1). The biological function of fluorescently labeled and non-labeled CSF-1 was assayed by macrophage differentiation from bone marrow cells (supplementary material Fig. S1).

BMM culture and retroviral transduction

mCit–Rab5a and YFP–Rab7 were cloned into an MoMLV-based retroviral cassette, PIB2-MCS, between the restriction sites *Mlu*I and *Nsi*I. BMMs were differentiated in DMEM supplemented with 20% heat-inactivated fetal bovine serum and 30% L929-cell-conditioned medium from C57BL/6 mice. The PIB2-MCS plasmids were transiently transfected into Plat-E packaging cells (Cell Biolabs, Inc.) using Fugene 6 (Roche Applied Sciences). Viral supernatant was collected

72 hours after transfection. For transduction, BMMs were exposed to viral supernatant for 72 hours in culture medium.

Isolation and differentiation of human monocytes from blood

Freshly drawn blood was diluted 1:1 in Dulbecco's phosphate-buffered saline (DPBS), layered on Ficoll-Paque (GE Healthcare) and centrifuged at 900 ***g*** for 20 minutes. Mononuclear cells at the interface were collected and washed three times in DPBS. Cells were plated at a density of 2×10^6 cells/ml on 10-cm culture dishes in complete growth medium (high-glucose DMEM containing 20% fetal bovine serum). After 4 hours, the medium was removed and adherent cells were washed with DPBS to remove non-adherent mononuclear cells. Remaining adherent mononuclear cells were cultured in growth medium supplemented with 5 ng/ml human CSF-1 for 7 days before imaging (medium was replaced every 48 hours).

siRNA

Small interfering (si)RNA (Smart Pool, Dharmacon) was used to knock down CHC in mouse BMMs. 1×10^6 D7 BMM cells were transfected with 100 pmol of siRNA using the mouse macrophage Nucleofector kit (Lonza), and the cells were re-transfected at day 3 after first transfection for double CHC knockdown. A transferrin uptake assay, using Alexa-Fluor-488-conjugated transferrin (Invitrogen), and a CSF-1R internalization assay were conducted at day 6 post-transfection. Western blot analysis was used to verify CHC knockdown.

Macropinosome quantification and manipulation of macropinocytosis

To measure macropinosome formation in response to CSF-1 stimulation, BMMs were starved of ligand overnight in DMEM supplemented with 10% fetal bovine serum. Cells were exposed to 100 ng/ml recombinant CSF-1 or 400 ng/ml CXCL12 in the presence of 0.5 mg/ml 70,000 Da TXR–Dex. Cells were washed and fixed with 4% paraformaldehyde (PFA) at 5 or 15 minutes, as specified in the figure legends. The macropinosome number per cell was quantified by counting all labeled vesicles in fluorescence images. The diameter for macropinosomes was quantified in ImageJ by line measurements across individual organelles in fluorescence images. Macropinosomes were assumed to be spheres, and volumes were calculated using the formula volume$=4/3\pi r^3$.

Acute blockade of macropinocytosis was achieved by pre-incubating BMM with either 0.5 µM latrunculin for 5 minutes or 75 µM blebbistatin for 10 minutes, followed by a 5-minute incubation with 1 µM jasplakinolide. All treatments were performed in a 5% CO_2 incubator at 37℃. The number of macropinosomes in drug-treated cells was quantified as described above.

Immunofluorescence

Following CSF-1 stimulation of starved BMMs for specific times, cells were fixed with 4% PFA for 10 minutes, permeabilized with 1 mg/ml Triton X-100 for 10 minutes at room temperature and blocked with 1% bovine serum albumin (BSA), each in a PBS buffer. Stimulation and chase steps were performed in a 5% CO_2 incubator at 37℃. Subsequent fixation and immunofluorescence steps were conducted at room temperature. Primary and secondary antibody incubations were each performed for 1 hour at room temperature. Surface-localized receptor staining was similar to the immunofluorescence protocol described above, except that cells were fixed with 2% PFA for 5 minutes and the cells were not permeabilized. Cells co-stained for CSF-1R and CXCR4 were fixed and permeabilized in methanol for 10 minutes at −20℃.

Antibodies recognizing CSF-1R extracellular or cytosolic epitopes were used to map the topology of the CSF-1R. Following CSF-1 stimulation for specific periods of time, cells were fixed with 2% PFA for 5 minutes at room temperature. The plasma membrane was selectively permeabilized by exposure of cells to 40 µg/ml digitonin for 30 seconds at room temperature. Following 1% BSA blocking at room temperature for 30 seconds, cells were incubated with two CSF-1R antibodies. Alexa-Fluor-488- and Dylight-594-conjugated secondary antibodies were used to specifically detect each primary antibody.

Sequential immunostaining of CSF-1R on macropinosomes was achieved on the Till iMic using an *x-y-z* positioning stage. BMMs were starved overnight and were stimulated with L929 cell supernatant plus 0.5 mg/ml TXR–Dex (70 kDa) for 15 minutes, fixed and mounted into an Attofluor cell chamber (Invitrogen). Several cells spanning ten fields of view were imaged in a single experiment by using an automated stage tracking *X*, *Y* and *Z* coordinates. Images were acquired following each stage of processing: fixation, permeabilization and immunostaining against CSF-1R.

Western blotting

Following CSF-1 stimulation, BMMs were lysed with mPer lysis buffer (Thermo Fisher) plus 1:100 proteinase inhibitor cocktail (Sigma) and 100 µM sodium orthovanadate (Sigma). Protein concentration was determined by using the bicinchoninic acid (BCA) assay. Following protein quantification, protein samples were separated by using the Mini-PROTEAN dual cell (BioRad) on 8% pre-cast Tris-Glycine NB gels (NuSep). Gels were transferred to nitrocellulose membranes using the Mini-PROTEAN dual cell (BioRad). Membranes were blocked for 1 hour at room temperature using 5% BSA and were incubated with primary antibody overnight at 4℃ or for 2 hours at room temperature. Membranes were imaged by using the LI-COR Odyssey infrared imaging system. Western blot images were quantified using ImageJ. For all experiments, protein values were normalized against an internal loading control (total Erk). For each experiment, CSF-1R intensity values for each data point were normalized against the intensity of the corresponding unstimulated sample.

Microscopy and data analysis

Immunofluorescence images were acquired on a Leica CTR4000 inverted microscope equipped with an QICAM 12-bit color camera, 12 V 100 W halogen lamp, QCapture software and 60× oil lens. Exposure times were optimized according to sample brightness. For quantification of immunofluorescence images in MATLAB (MathWorks), imaging parameters were held constant for each experimental condition. A binary mask was created using threshholding. Intensity was calculated on a per cell basis. Only regions of the image in which whole cells were evident were measured.

Live-cell imaging and the sequential dextran immunofluorescence experiments were performed on a custom-built Till iMic microscope (FEI) using a 60× water lens (a complete schematic of the imaging system can be found in Hoppe et al., 2013). Macrophages starved of CSF-1 overnight were pulsed with 100 ng/ml TXR–CSF-1 for 1 minute, washed and chased for 14 minutes. Images were taken before the pulse and chase with CSF-1 on both yellow and red channels at a rate of 20 seconds between frames. Red and yellow channel images were registered and normalized. A colocalization coefficient between yellow and red images was calculated according to the Pearson correlation coefficient in MATLAB.

Acknowledgements

We thank Lu Huang, Shuangling Zhang and Dakota Weathers for technical assistance and Geoffrey Graff for the drawing in Fig. 7.

Competing interests

The authors declare no competing interests.

Author contributions

J.L. and A.D.H designed the study. J.L, S.T.L.-N. and J.G.K. conducted the experiments and analyzed the data. J.L. and A.D.H. wrote the manuscript.

Funding

This work was supported by the South Dakota Governor's 2010 center for the Biological Control and Analysis by Applied Photonics (BCAAP); South Dakota State University Chemistry and Biochemistry startup funds to A.D.H.; and a National Institutes of Health fellowship [grant number 1F32GM105277] to S.T.L.-N. Deposited in PMC for release after 12 months.

Supplementary material

Supplementary material available online at
http://jcs.biologists.org/lookup/suppl/doi:10.1242/jcs.154393/-/DC1

References

Amyere, M., Payrastre, B., Krause, U., Van Der Smissen, P., Veithen, A. and Courtoy, P. J. (2000). Constitutive macropinocytosis in oncogene-transformed fibroblasts depends on sequential permanent activation of phosphoinositide 3-kinase and phospholipase C. *Mol. Biol. Cell* **11**, 3453-3467.

Araki, N., Johnson, M. T. and Swanson, J. A. (1996). A role for phosphoinositide 3-kinase in the completion of macropinocytosis and phagocytosis by macrophages. *J. Cell Biol.* **135**, 1249-1260.

Boocock, C. A., Jones, G. E., Stanley, E. R. and Pollard, J. W. (1989). Colony-stimulating factor-1 induces rapid behavioural responses in the mouse macrophage cell line, BAC1.2F5. *J. Cell Sci.* **93**, 447-456.

Braun, V., Fraisier, V., Raposo, G., Hurbain, I., Sibarita, J. B., Chavrier, P., Galli, T. and Niedergang, F. (2004). TI-VAMP/VAMP7 is required for optimal phagocytosis of opsonised particles in macrophages. *EMBO J.* **23**, 4166-4176.

Chen, B. D. and Lin, H. S. (1984). Colony-stimulating factor (CSF-1): its enhancement of plasminogen activator production and inhibition of cell growth in a mouse macrophage cell line. *J. Immunol.* **132**, 2955-2960.

Clarke, M. and Kayman, S. C. (1987). The axenic mutations and endocytosis in Dictyostelium. *Methods Cell Biol.* **28**, 157-176.

Commisso, C., Davidson, S. M., Soydaner-Azeloglu, R. G., Parker, S. J., Kamphorst, J. J., Hackett, S., Grabocka, E., Nofal, M., Drebin, J. A., Thompson, C. B. et al. (2013). Macropinocytosis of protein is an amino acid supply route in Ras-transformed cells. *Nature* **497**, 633-637.

Dutta, D., Williamson, C. D., Cole, N. B. and Donaldson, J. G. (2012). Pitstop 2 is a potent inhibitor of clathrin-independent endocytosis. *PLoS ONE* **7**, e45799.

Feliciano, W. D., Yoshida, S., Straight, S. W. and Swanson, J. A. (2011). Coordination of the Rab5 cycle on macropinosomes. *Traffic* **12**, 1911-1922.

Fujii, M., Kawai, K., Egami, Y. and Araki, N. (2013). Dissecting the roles of Rac1 activation and deactivation in macropinocytosis using microscopic photo-manipulation. *Sci. Rep.* **3**, 2385.

Goh, L. K., Huang, F., Kim, W., Gygi, S. and Sorkin, A. (2010). Multiple mechanisms collectively regulate clathrin-mediated endocytosis of the epidermal growth factor receptor. *J. Cell Biol.* **189**, 871-883.

Hewlett, L. J., Prescott, A. R. and Watts, C. (1994). The coated pit and macropinocytic pathways serve distinct endosome populations. *J. Cell Biol.* **124**, 689-703.

Hoppe, A. D., Scott, B. L., Welliver, T. P., Straight, S. W. and Swanson, J. A. (2013). N-way FRET microscopy of multiple protein-protein interactions in live cells. *PLoS ONE* **8**, e64760.

Hurley, J. H. and Emr, S. D. (2006). The ESCRT complexes: structure and mechanism of a membrane-trafficking network. *Annu. Rev. Biophys. Biomol. Struct.* **35**, 277-298.

Huynh, J., Kwa, M. Q., Cook, A. D., Hamilton, J. A. and Scholz, G. M. (2012). CSF-1 receptor signalling from endosomes mediates the sustained activation of Erk1/2 and Akt in macrophages. *Cell. Signal.* **24**, 1753-1761.

Kerr, M. C. and Teasdale, R. D. (2009). Defining macropinocytosis. *Traffic* **10**, 364-371.

Koivusalo, M., Welch, C., Hayashi, H., Scott, C. C., Kim, M., Alexander, T., Touret, N., Hahn, K. M. and Grinstein, S. (2010). Amiloride inhibits macropinocytosis by lowering submembranous pH and preventing Rac1 and Cdc42 signaling. *J. Cell Biol.* **188**, 547-563.

Laplante, M. and Sabatini, D. M. (2012). mTOR signaling in growth control and disease. *Cell* **149**, 274-293.

Lee, P. S., Wang, Y., Dominguez, M. G., Yeung, Y. G., Murphy, M. A., Bowtell, D. D. and Stanley, E. R. (1999). The Cbl protooncoprotein stimulates CSF-1 receptor multiubiquitination and endocytosis, and attenuates macrophage proliferation. *EMBO J.* **18**, 3616-3628.

Lemmon, M. A. and Schlessinger, J. (2010). Cell signaling by receptor tyrosine kinases. *Cell* **141**, 1117-1134.

Macia, E., Ehrlich, M., Massol, R., Boucrot, E., Brunner, C. and Kirchhausen, T. (2006). Dynasore, a cell-permeable inhibitor of dynamin. *Dev. Cell* **10**, 839-850.

Maekawa, M., Terasaka, S., Mochizuki, Y., Kawai, K., Ikeda, Y., Araki, N., Skolnik, E. Y., Taguchi, T. and Arai, H. (2014). Sequential breakdown of 3-phosphorylated phosphoinositides is essential for the completion of macropinocytosis. *Proc. Natl. Acad. Sci. USA* **111**, E978-E987.

Mercer, J., Schelhaas, M. and Helenius, A. (2010). Virus entry by endocytosis. *Annu. Rev. Biochem.* **79**, 803-833.

Murray, J., Wilson, L. and Kellie, S. (2000). Phosphatidylinositol-3′ kinase-dependent vesicle formation in macrophages in response to macrophage colony stimulating factor. *J. Cell Sci.* **113**, 337-348.

Norbury, C. C. (2006). Drinking a lot is good for dendritic cells. *Immunology* **117**, 443-451.

Park, R. J., Shen, H., Liu, L., Liu, X., Ferguson, S. M. and De Camilli, P. (2013). Dynamin triple knockout cells reveal off target effects of commonly used dynamin inhibitors. *J. Cell Sci.* **126**, 5305-5312.

Philippidou, P., Valdez, G., Akmentin, W., Bowers, W. J., Federoff, H. J. and Halegoua, S. (2011). Trk retrograde signaling requires persistent, Pincher-directed endosomes. *Proc. Natl. Acad. Sci. USA* **108**, 852-857.

Pixley, F. J. and Stanley, E. R. (2004). CSF-1 regulation of the wandering macrophage: complexity in action. *Trends Cell Biol.* **14**, 628-638.

Polo, S. and Di Fiore, P. P. (2006). Endocytosis conducts the cell signaling orchestra. *Cell* **124**, 897-900.

Porat-Shliom, N., Kloog, Y. and Donaldson, J. G. (2008). A unique platform for H-Ras signaling involving clathrin-independent endocytosis. *Mol. Biol. Cell* **19**, 765-775.

Racoosin, E. L. and Swanson, J. A. (1992). M-CSF-induced macropinocytosis increases solute endocytosis but not receptor-mediated endocytosis in mouse macrophages. *J. Cell Sci.* **102**, 867-880.

Racoosin, E. L. and Swanson, J. A. (1993). Macropinosome maturation and fusion with tubular lysosomes in macrophages. *J. Cell Biol.* **121**, 1011-1020.

Raiborg, C. and Stenmark, H. (2009). The ESCRT machinery in endosomal sorting of ubiquitylated membrane proteins. *Nature* **458**, 445-452.

Rink, J., Ghigo, E., Kalaidzidis, Y. and Zerial, M. (2005). Rab conversion as a mechanism of progression from early to late endosomes. *Cell* **122**, 735-749.

Schmees, C., Villaseñor, R., Zheng, W., Ma, H., Zerial, M., Heldin, C. H. and Hellberg, C. (2012). Macropinocytosis of the PDGF β-receptor promotes fibroblast transformation by H-RasG12V. *Mol. Biol. Cell* **23**, 2571-2582.

Scholl, S. M., Bascou, C. H., Mosseri, V., Olivares, R., Magdelenat, H., Dorval, T., Palangié, T., Validire, P., Pouillart, P. and Stanley, E. R. (1994). Circulating levels of colony-stimulating factor 1 as a prognostic indicator in 82 patients with epithelial ovarian cancer. *Br. J. Cancer* **69**, 342-346.

Sigismund, S., Argenzio, E., Tosoni, D., Cavallaro, E., Polo, S. and Di Fiore, P. P. (2008). Clathrin-mediated internalization is essential for sustained EGFR signaling but dispensable for degradation. *Dev. Cell* **15**, 209-219.

Sorkin, A. and Goh, L. K. (2009). Endocytosis and intracellular trafficking of ErbBs. *Exp. Cell Res.* **315**, 683-696.

Sorkin, A. and von Zastrow, M. (2009). Endocytosis and signalling: intertwining molecular networks. *Nat. Rev. Mol. Cell Biol.* **10**, 609-622.

Swanson, J. A. (2008). Shaping cups into phagosomes and macropinosomes. *Nat. Rev. Mol. Cell Biol.* **9**, 639-649.

Valdez, G., Akmentin, W., Philippidou, P., Kuruvilla, R., Ginty, D. D. and Halegoua, S. (2005). Pincher-mediated macroendocytosis underlies retrograde signaling by neurotrophin receptors. *J. Neurosci.* **25**, 5236-5247.

Valdez, G., Philippidou, P., Rosenbaum, J., Akmentin, W., Shao, Y. and Halegoua, S. (2007). Trk-signaling endosomes are generated by Rac-dependent macroendocytosis. *Proc. Natl. Acad. Sci. USA* **104**, 12270-12275.

Veltman, D. M., Lemieux, M. G., Knecht, D. A. and Insall, R. H. (2014). PIP_3-dependent macropinocytosis is incompatible with chemotaxis. *J. Cell Biol.* **204**, 497-505.

von Kleist, L., Stahlschmidt, W., Bulut, H., Gromova, K., Puchkov, D., Robertson, M. J., MacGregor, K. A., Tomilin, N., Pechstein, A., Chau, N. et al. (2011). Role of the clathrin terminal domain in regulating coated pit dynamics revealed by small molecule inhibition. *Cell* **146**, 471-484.

von Zastrow, M. and Sorkin, A. (2007). Signaling on the endocytic pathway. *Curr. Opin. Cell Biol.* **19**, 436-445.

Wang, Y., Yeung, Y. G. and Stanley, E. R. (1999). CSF-1 stimulated multiubiquitination of the CSF-1 receptor and of Cbl follows their tyrosine phosphorylation and association with other signaling proteins. *J. Cell. Biochem.* **72**, 119-134.

Welliver, T. P., Chang, S. L., Linderman, J. J. and Swanson, J. A. (2011). Ruffles limit diffusion in the plasma membrane during macropinosome formation. *J. Cell Sci.* **124**, 4106-4114.

Willox, A. K., Sahraoui, Y. M. and Royle, S. J. (2014). Non-specificity of Pitstop 2 in clathrin-mediated endocytosis. *Biol. Open* **3**, 326-331.

Xiong, Y., Song, D., Cai, Y., Yu, W., Yeung, Y. G. and Stanley, E. R. (2011). A CSF-1 receptor phosphotyrosine 559 signaling pathway regulates receptor ubiquitination and tyrosine phosphorylation. *J. Biol. Chem.* **286**, 952-960.

Yeung, Y. G., Wang, Y., Einstein, D. B., Lee, P. S. and Stanley, E. R. (1998). Colony-stimulating factor-1 stimulates the formation of multimeric cytosolic complexes of signaling proteins and cytoskeletal components in macrophages. *J. Biol. Chem.* **273**, 17128-17137.

Yoshida, S., Hoppe, A. D., Araki, N. and Swanson, J. A. (2009). Sequential signaling in plasma-membrane domains during macropinosome formation in macrophages. *J. Cell Sci.* **122**, 3250-3261.

Yu, W., Chen, J., Xiong, Y., Pixley, F. J., Dai, X. M., Yeung, Y. G. and Stanley, E. R. (2008). CSF-1 receptor structure/function in MacCsf1r-/- macrophages: regulation of proliferation, differentiation, and morphology. *J. Leukoc. Biol.* **84**, 852-863.

Yu, W., Chen, J., Xiong, Y., Pixley, F. J., Yeung, Y. G. and Stanley, E. R. (2012). Macrophage proliferation is regulated through CSF-1 receptor tyrosines 544, 559, and 807. *J. Biol. Chem.* **287**, 13694-13704.

SUPPLEMENT

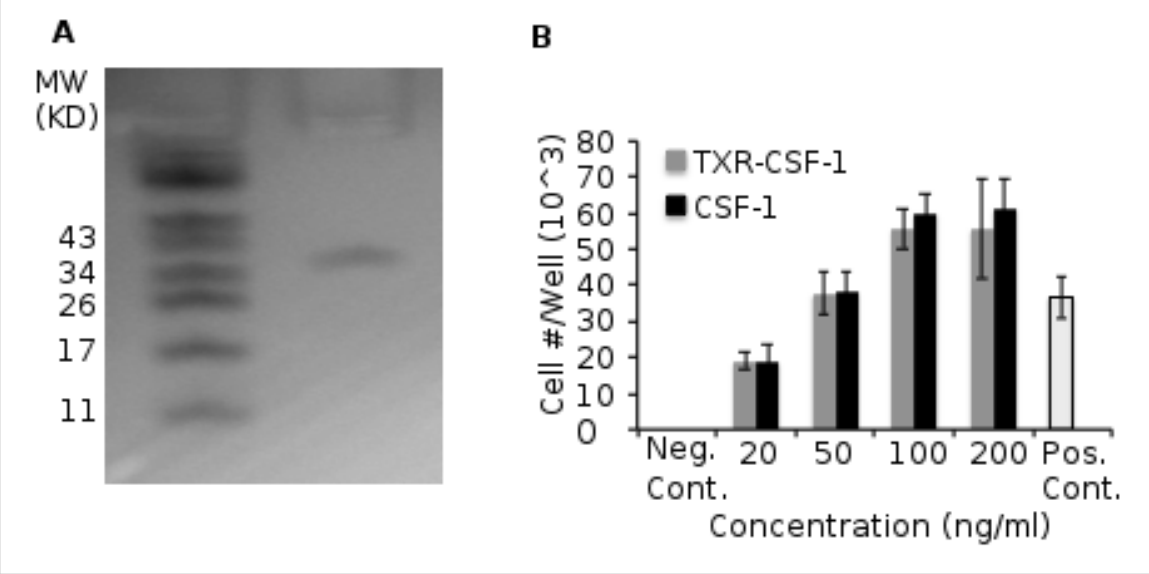

S Figure1. **Texas red labeled recombinant human CSF-1 (TXR-CSF-1) has the same biological activity as non-labeled CSF-1. a.** SDS-PAGE showed pure CSF-1 dimer (MW 34 KDa). **b.** Both CSF-1 and TXR-CSF-1 are both competent for bone marrow macrophage differentiation. Positive control is the number of bone marrow macrophage cultured by L cell supernatant added bone marrow medium.

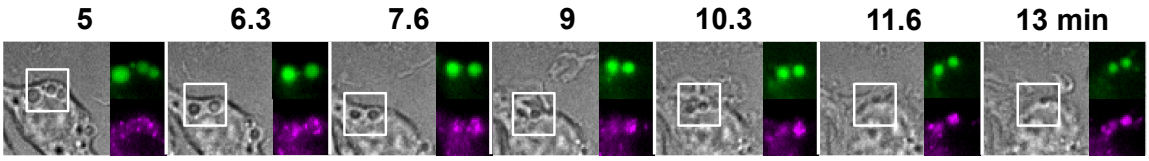

Figure S2. Traffic to the CSF-1R to macropinosomes labeled with the fluid phase marker Lucifer Yellow. Live BMM were exposed to Dylight 594-CSF-1 and Lucifer Yellow (LY) 5 minutes and imaged. Dylight 594-CSF-1 associated with LY positive macropinosomes at 5 minutes and was delivered into the lumen around ~8 min.

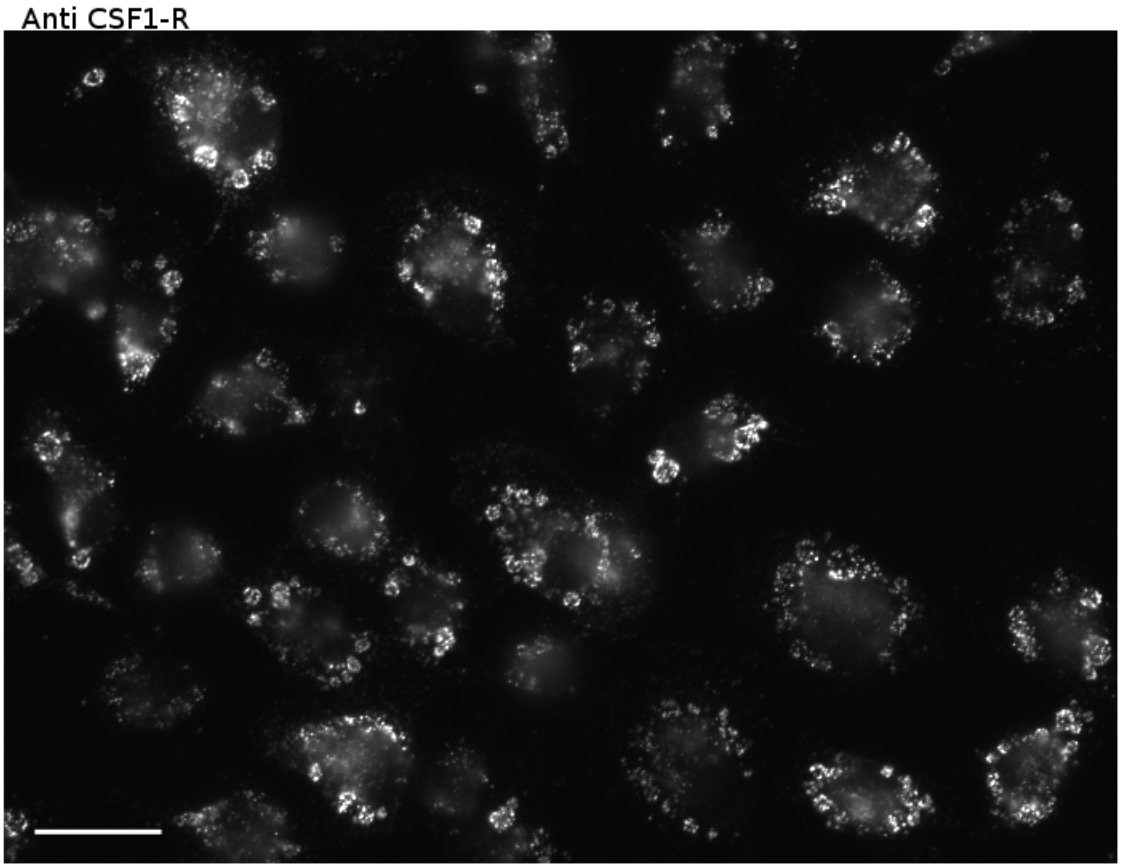

Figure S3. Generality of the observation that the CSF-1R is delivered to macropinosomes after exposure to CSF-1 for 15 min. The localization and distribution of CSF-1R was followed by immunofluorescence after stimulating BMM with 100 ng/ml CSF-1 for 15 min. Most CSF-1R clustered and appeared as large circular structures (macropinosomes) that contained many small puncta (scale bar = 10 μm).

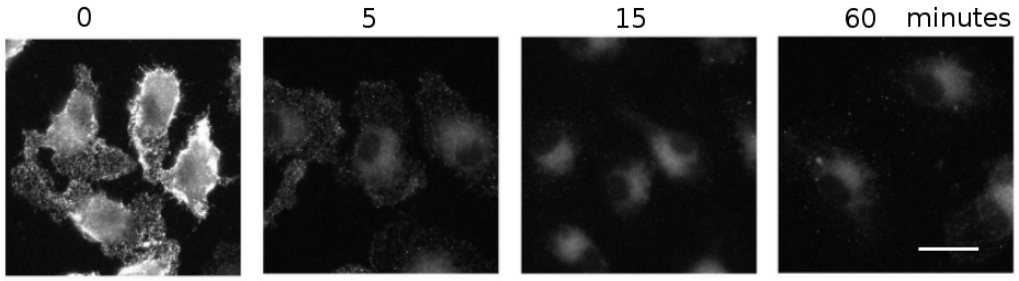

Figure S4. No detectable CSF-1R is recycled back to cell surface. Immunofluorescence against the cell surface CSF-1R in BMM showed that the CSF-1R is internalized by 15 min. following exposure to 100 ng/ml MCSF for 15 minutes and there is minimum amount of receptors been recycled. (scale bar = 5 μm)

Movie 1. CSF-1 induced ruffling and macropinocytosis in BMM. CSF-1 stimulated ruffling and macropinocytosis in BMM. BMM starved of CSF-1 overnight were exposed to 100 ng/mL for 1 minute (3rd frame) after the start of the acquisition. Note the formation of circular ruffles that close to form macropinosomes. Images were acquired at a rate of 1 frame every 20 seconds for a total of 15 minutes (playback is 150× real time).

Movie 2. TXR-CSF-1 traffic to macropinosomes. BMM were exposed to CSF- to 100 ng/mL TXR-CSF-1 1 minute after the start of the acquisition (white frames). TXR-CSF-1 is internalized by small vesicles that undergo homotypic fusion and then traffic to macropinosomes (large ring like structures), whereupon the TXR-CSF-1 is delivered to the lumen (large circles of fluorescence). The cell in white box is also shown in Fig. 1. Duration was 17 minutes at a frame rate of 1 frame every 20 seconds, playback speed is 100 times real time.

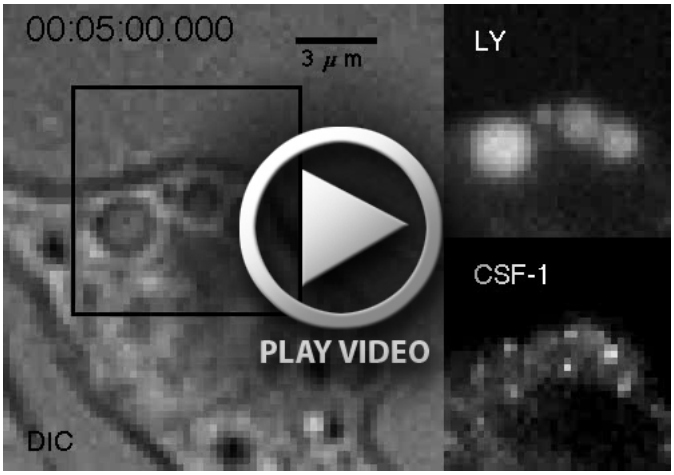

Movie 3. CSF-1 traffics to nascent macropinosomes marked by Lucifer Yellow. BMM stimulated with 100 ng/mL DiLight594-CSF-1, in the presence of Lucifer Yellow (LY), for 5 minutes prior to imaging. Macropinosomes, visible in DIC, were tracked in the black boxed region in DIC image. These macropinosomes contained LY when formed and accumulated DiLight594-CSF-1 over the time. Images were acquired at a rate of 1 frame every 20 seconds (playback is 45× real time).

Movie 4. Selective permeabilization of BMM plasma membrane. Macrophages expressing cytosolic mCerulean were stimulated with 100 ng/mL CSF-1, in the presence of 0.5 mg/mL TXR-Dex (70,000 MW), for 5 minutes prior to imaging. Digitonin (40 μg/mL) and 0.1% TritonX-100 were added at the times indicated, resulting in the loss of mCerulean from the cytosol (Digitonin) and subsequent loss of TXR-Dex from the macropinosome (TritonX-100). Images were acquired at a rate of 1 frame every 2 seconds (playback is 7× real time).

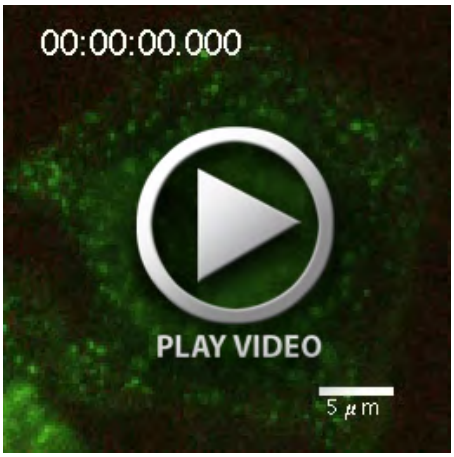

Movie 5. CSF-1-containing vesicles fuse with Rab5-positive macropinosomes. BMM expressing mCit-Rab5a (green) were exposed to TXR-CSF-1 (red) 1 minute after the start of the acquisition (yellow frames). Initially, small endosomes bearing TXR-CSF-1 localized with mCit-Rab5a. Newly formed macropinosomes acquire mCit-Rab5a (large green rings) and subsequently TXR-CSF-1 laden vesicles. Images from this sequence are shown in Fig. 3. Duration is 17 minutes, 1 frame every 20 s, playback is 100× real time.